Journal of Molecular Graphics and Modelling 41 (2013) 31–42

Contents lists available at SciVerse ScienceDirect

Journal of Molecular Graphics and Modelling

journal homepage: www.elsevier.com/locate/JMGM

Three- and four-body corrected fragment molecular orbital calculations with a novel subdividing fragmentation method applicable to structure-based drug design

Chiduru Watanabe[a,*], Kaori Fukuzawa[a,b], Yoshio Okiyama[a], Takayuki Tsukamoto[a,b], Akifumi Kato[b], Shigenori Tanaka[c], Yuji Mochizuki[a,d], Tatsuya Nakano[a,e]

[a] Institute of Industrial Science, The University of Tokyo, 4-6-1 Komaba, Meguro-ku, Tokyo 153-8505, Japan
[b] Mizuho Information & Research Institute Inc., 2-3 Kanda Nishiki-Cho, Chiyoda-ku, Tokyo 101-8443, Japan
[c] Graduate School of System Informatics, Department of Computational Science, Kobe University, 1-1 Rokkodai, Nada, Kobe 657-8501, Japan
[d] Department of Chemistry & Research Center for Smart Molecules, Faculty of Science, Rikkyo University, 3-34-1 Nishi-Ikebukuro, Toshima-ku, Tokyo 171-8501, Japan
[e] Division of Medicinal Safety Science, National Institute of Health Sciences, 1-18-1 Kamiyouga, Setagaya-ku, Tokyo 158-8501, Japan

ARTICLE INFO

Article history:
Accepted 25 January 2013
Available online 8 February 2013

Keywords:
Four-body corrected fragment molecular orbital (FMO4) method
Four-body corrected inter-fragment interaction energy (FMO4-IFIE)
Ligand fragmentation
Protein–ligand interaction
Structure-based drug design (SBDD)
CH/π interaction

ABSTRACT

We develop an inter-fragment interaction energy (IFIE) analysis based on the three- and four-body corrected fragment molecular orbital (FMO3 and FMO4) method to evaluate the interactions of functional group units in structure-based drug design context. The novel subdividing fragmentation method for a ligand (in units of their functional groups) and amino acid residues (in units of their main and side chains) enables us to understand the ligand-binding mechanism in more detail without sacrificing chemical accuracy of the total energy and IFIEs by using the FMO4 method. We perform FMO4 calculations with the second order Møller-Plesset perturbation theory for an estrogen receptor (ER) and the 17β-estradiol (EST) complex using the proposed fragmentation method and assess the interaction for each ligand-binding site by the FMO4-IFIE analysis. When the steroidal EST is divided into two functional units including "A ring" and "D ring", respectively, the FMO4-IFIE analysis reveals their binding affinity with surrounding fragments of the amino acid residues; the "A ring" of EST has polarization interaction with the main chain of Thr347 and two hydrogen bonds with the side chains of Glu353 and Arg394; the "D ring" of EST has a hydrogen bond with the side chain of His524. In particular, the CH/π interactions of the "A ring" of EST with the side chains of Leu387 and Phe404 are easily identified in cooperation with the CHPI program. The FMO4-IFIE analysis using our novel subdividing fragmentation method, which provides higher resolution than the conventional IFIE analysis in units of ligand and each amino acid reside in the framework of two-body approximation, is a useful tool for revealing ligand-binding mechanism and would be applicable to rational drug design such as structure-based drug design and fragment-based drug design.

1. Introduction

The fragment molecular orbital (FMO) method, which has been proposed by Kitaura et al., enables us to efficiently perform *ab initio* quantum mechanical calculations for several large biomolecules with reduced computational costs [1–5]. In the FMO method, such large biomolecules are divided into smaller fragments and the molecular orbital (MO) calculations for these fragments (monomers) and fragment pairs (dimers) are performed to obtain the total energy, which is expressed as a sum of the fragment energies and the inter-fragment interaction energies (IFIEs). The IFIE analysis is one of the advantages of the FMO method because it can easily represent the detailed interactions in units of a ligand and each amino acid residue [6–12]. Thus, IFIE analysis is a helpful tool for drug design, and it is now widely used in the development of new drugs [13–20]. The IFIE analysis based on the FMO method has been used to reveal the ligand-binding mechanism of the estrogen receptor (ER), which is an important drug target for breast cancer and other diseases [21–25].

Whereas fragmentation in units of a ligand and each amino acid residue is recommended when using the two-body FMO (FMO2) method, the evaluation of IFIEs for each ligand-binding site at the functional unit (i.e., fragmentation of the ligand) is more desirable from the point of view of structure-based drug design (SBDD) [26–28]. Because the natural ligand, 17β-estradiol (EST), primarily binds to two sites of the ER (Glu353, Arg394, and His524) by

* Corresponding author. Tel.: +81 3 5452 6622; fax: +81 3 5452 6662.
E-mail address: chiduru@iis.u-tokyo.ac.jp (C. Watanabe).

1093-3263/$ – see front matter © 2013 Elsevier Inc. All rights reserved.
http://dx.doi.org/10.1016/j.jmgm.2013.01.006

hydrogen-bonds, these interactions must be analyzed individually by substructure or functional group unit so as to elucidate the mechanism by which the ligand binds with the ER. Hitaoka et al. attempted IFIE analysis between neuraminidase-1 (N1-NA) and an inhibitor with ligand fragmentation [29,30]. They emphasized the importance of using ligand fragmentation for the development of new high-potency drugs. The IFIEs at functional units of the inhibitor, which were obtained by FMO2 calculation at the second order Møller-Plesset perturbation (MP2) level, revealed that the charged and hydrophobic groups cause complex formations and variations in the inhibitory potency, respectively. In the two-body approximation framework, however, ligand fragmentation is not sufficient to calculate the intermolecular interactions of each ligand-binding site with chemical accuracy.

Umezawa and Nishio reported that not only electrostatic interactions, such as hydrogen bonds, but also weak dispersion interactions, such as CH/π hydrogen bonds in units of functional groups, would play key roles in protein-ligand binding mechanisms and the folding of proteins in biomolecular systems [31–36]. Whereas CH/π hydrogen bonds can be easily searched for structurally by using the CHPI program [31,37], quantitative estimates of CH/π interactions require a fragment interaction analysis based on local MP2 (FILM) [38], which can estimate the electron correlation energy for dispersion interactions at the molecular orbital level. FILM contains a great deal of interaction information regarding orbital pairs; however, compared with IFIE analysis, FILM is too complicated to yield an intuitive understanding. Conversely, IFIE analysis using large fragments, such as amino acid residue units, is still too coarse to be used to determined local CH/π interactions. To evaluate CH/π interaction by IFIE analysis, we need to separate functional group with π orbital as an individual fragment (e.g., Phe, Trp, and ligand including aromatic ring). Recently, the four-body corrected fragment molecular orbital (FMO4) method [39] was developed and applied with high accuracy to the subdivision of amino acid residue fragments into smaller main and side chain fragments. Using this method, we attempt to perform the FMO4 calculation by using the fragmentation of a ligand to distinguish each functional group and the fragmentation of a protein divided into main and side chains.

In this study, we demonstrate the importance of the four-body corrected IFIEs (FMO4-IFIEs) by using a novel subdividing fragmentation method for a ligand and amino acid residues to evaluate the critical intermolecular interactions in units of substructure and functional groups, which are important for rational drug design methods such as SBDD and fragment-based drug design (FBDD) [40,41]. We analyze the FMO4-IFIEs between the ER and EST by using our novel subdividing fragmentation method while maintaining chemical accuracy. In the first part of this paper, we examine the accuracy of the total energy and IFIE values by using two-, three-, and four-body corrections with the novel subdividing fragmentation method, where the steroidal EST is divided into two functional units including “A ring” and “D ring”, respectively. In the second part of this paper, we explore FMO4-IFIEs between the ER and EST for each ligand-binding site and reveal binding affinity in functional units of EST. Moreover, we identify CH/π interactions by combining the FMO4-IFIE analysis with our novel subdividing fragmentation method and the CHPI program.

2. Computational methods

2.1. Four-body corrected fragment orbital (FMO4) method

To briefly describe the *ab initio* FMO4 method [39], a molecule or a molecular cluster is divided into small fragments and the MO calculations on each fragment monomer, dimer, trimer, and tetramer are performed to obtain the properties of the entire system. The many-body effects are considered through the environmental electrostatic potential (ESP). The total energies of the FMO2, FMO3, and FMO4 methods are given by

$$E_{\text{total}}^{\text{FMO2}} = \sum_I E_I' + \sum_{I>J} \Delta\tilde{E}_{IJ}, \tag{1}$$

$$E_{\text{total}}^{\text{FMO3}} = E_{\text{total}}^{\text{FMO2}} + \sum_{I>J>K} \Delta\tilde{E}_{IJK}, \tag{2}$$

$$E_{\text{total}}^{\text{FMO4}} = E_{\text{total}}^{\text{FMO3}} + \sum_{I>J>K>L} \Delta\tilde{E}_{IJKL}, \tag{3}$$

where E_I' is monomer energy without the environmental ESP; $\Delta\tilde{E}_{IJ}$, $\Delta\tilde{E}_{IJK}$, and $\Delta\tilde{E}_{IJKL}$ are two-, three-, and four-body inter-fragment interaction energies; and I, J, K, and L are fragment indices.

The inter-fragment interaction energies of two-, three-, and four-body corrections (FMOn-IFIEs, where $n = 2$, 3, and 4) are represented by

$$\Delta E_{IJ}^{\text{FMO2}} = \Delta\tilde{E}_{IJ}, \tag{4}$$

$$\Delta E_{IJ}^{\text{FMO3}} = \Delta E_{IJ}^{\text{FMO2}} + \frac{1}{3}\sum_K \Delta\tilde{E}_{IJK}, \tag{5}$$

$$\Delta E_{IJ}^{\text{FMO4}} = \Delta E_{IJ}^{\text{FMO3}} + \frac{1}{6}\sum_{KL} \Delta\tilde{E}_{IJKL}. \tag{6}$$

Sums of FMOn-IFIEs (FMOn-IFIE sums) on I-th fragment are defined by

$$\Delta E_I^{\text{FMO}n} = \sum_J \Delta E_{IJ}^{\text{FMO}n} \ (n = 2, 3, 4). \tag{7}$$

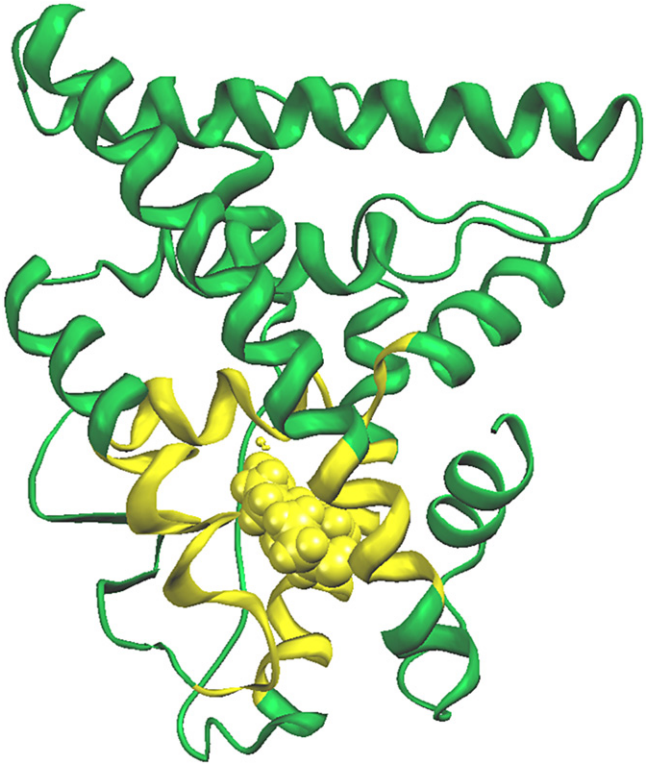

Fig. 1. Complex between the ER and EST. The model protein (which is composed 50 residues) is colored in yellow. (For interpretation of the references to color in the artwork, the reader is referred to the web version of the article.)

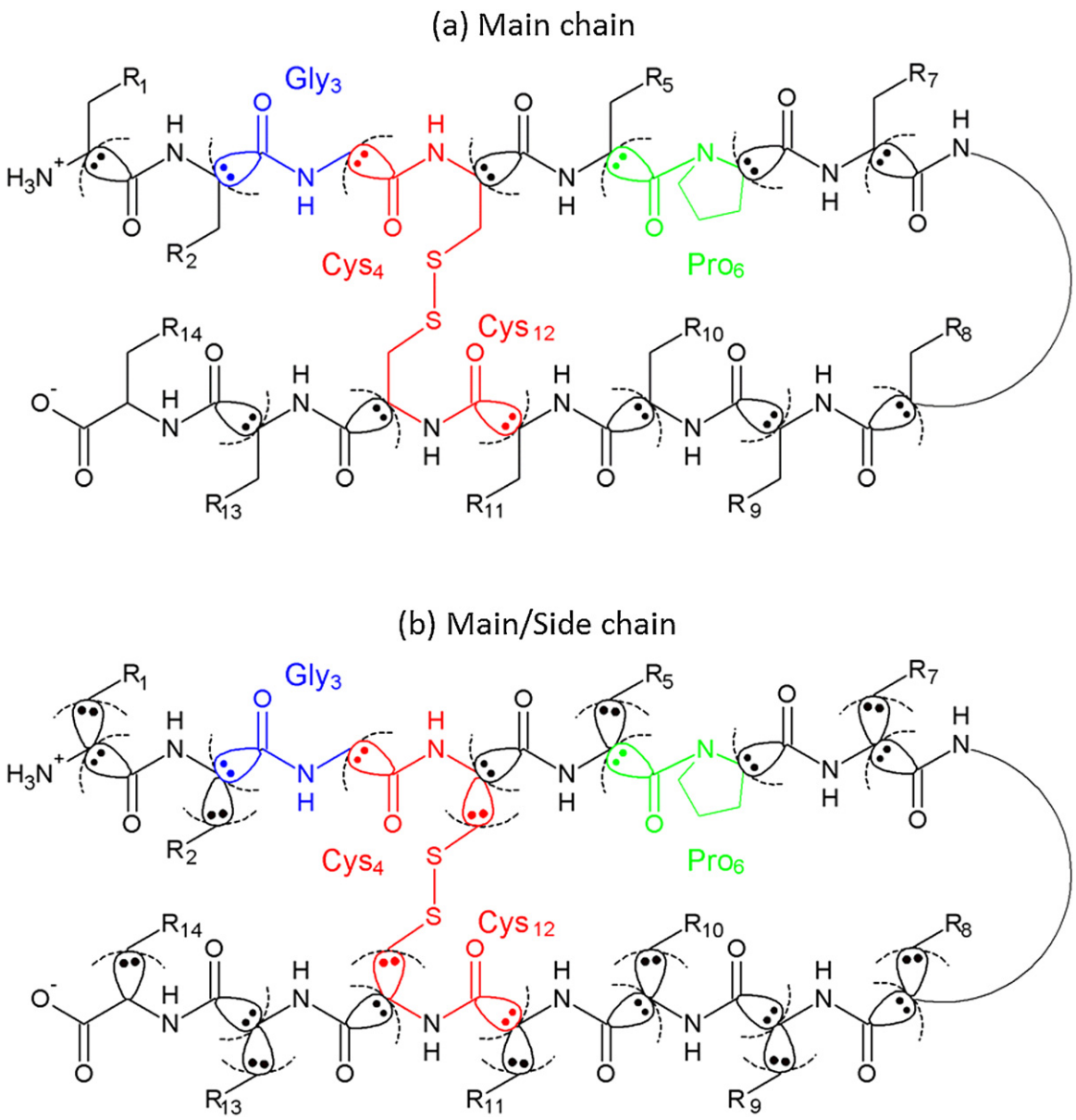

Fig. 2. Fragmentations of a protein: (a) conventional main chain fragmentation, (b) main/side chain fragmentation.

The FMO*n*-IFIE sums (where $n = 2$, 3, and 4) are used as an indicator of FMO*n*-IFIE quality to verify the calculation accuracy.

We demonstrate that FMO4-IFIE analysis is able to identify several ligand-binding sites of the ER–EST complex, which has been previously analyzed using the two-body approximation [7], by using a novel subdividing fragmentation method. To reduce computational costs, we use a minimum model protein composed of EST [6], a water molecule, and 50 residues of the ER around EST (residues 342–354, 382–395, 403–405, 417–429, and 520–526), as shown in Fig. 1. As the initial structure of complex between human ERαLBD and its agonist (EST), we use the coordinates available in the Protein Data Bank (PDB) entry 1ERE. The geometry optimization of the whole complex by CHARMM force field is performed only for the added hydrogen atoms with all heavy atoms fixed at the positions given in the PDB data, and the minimum model protein is clipped from the whole complex thereafter. In addition, the geometries of the water molecule and hydrogen atoms that constitute the hydrogen bond network between ER (the side chains of Glu353, Arg394, and His524, and the main chain of Leu387) and EST (two pieces of A and D ring) are optimized at the Hartree-Fock (HF) level with 6-31G(d) basis set. Finally, the atomic coordinates of the minimum model protein are replaced with the corresponding optimized hydrogen network model. For more information on this modeling and optimization of the minimum model protein for ER–EST complex, refer to a report by Fukuzawa et al. [6]. We perform FMO4 calculations at the HF and MP2 levels using the 6-31G basis set (HF/6-31G and MP2/6-31G) based on the novel subdividing fragmentations of the protein and ligand (Figs. 2 and 3) by using ABINIT-MPX program [3,42,43]. More detailed descriptions of the novel subdividing fragmentation method are given in section 2.2. In these calculations, we avoid using the approximations of ESP-PTC and ESP-AOC [3] to make clear comparisons with reference values obtained using conventional fragmentation and to maintain the consistency of the ESPs for each two-, three-, and four-body term. In addition, to compare with the conventional MO calculation, the FMO4 and MO calculations are performed under gas-phase conditions at the HF level using the STO-3G basis set (HF/STO-3G). The FMO4 calculations were performed on the Dell PowerEdge R620 clusters with Intel Xeon dual octal-core by using eight nodes (128 CPUs). The elapsed time was 45275.3 s for the

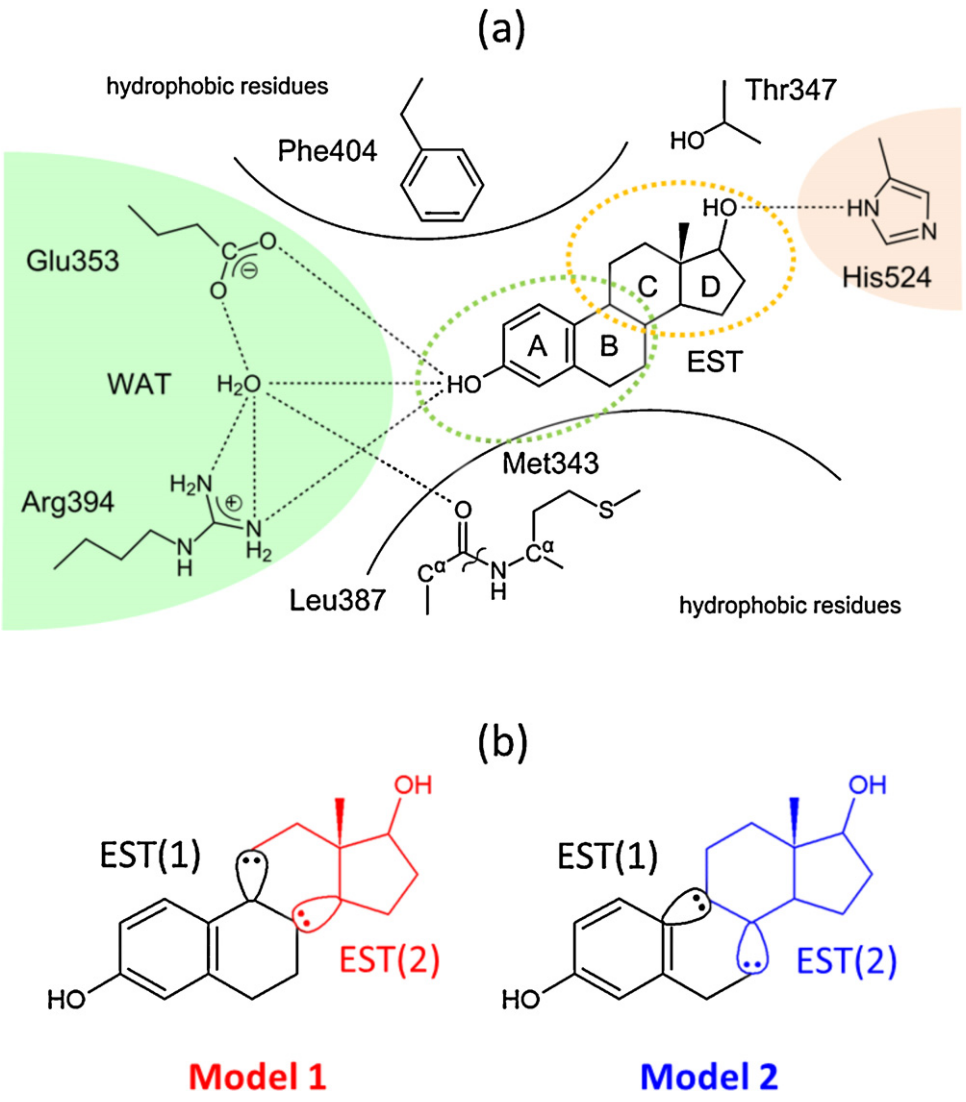

Fig. 3. (a) Ligand-binding network of the ER–EST complex and (b) ligand fragmentations for EST (Model 1 and Model 2). Dotted lines indicate hydrogen bonds in (a).

FMO4-MP2/6-31G calculations with conventional main chain fragmentation and 29355.3 s for the FMO4-MP2/6-31G calculations with the novel subdividing fragmentation method (main/side chain fragment and ligand fragmentation of Model 1). In this model protein of ER–EST complex (50 residues), the computational cost of the FMO4 calculation is reduced by miniaturization of fragment under the novel subdividing fragmentation method as compared to conventional fragmentation. The incremental costs of the FMO3 and FMO4 calculations with the novel subdividing fragmentation relative to the FMO2 calculation were observed to be about 3.5 and 10.2 times, respectively, for this model protein. On the other hand, these costs are about 1.0 and 3.1 times of the conventional scheme using FMO2 method with main chain fragmentation. The many-body IFIEs between each functional group of amino acid residues of the ER and each substructure of EST used for the FMO2, FMO3, and FMO4 calculations are analyzed by using a development version of BioStation Viewer [43].

2.2. A novel subdividing fragmentation method applicable to SBDD

In the pharmacophore of ER-EST complex, the hydrogen bonds play an important role for ligand-binding and the network is classified into two binding sites: Glu353 and Arg394 bind to a hydroxy group of the steroid "A ring" of EST through hydrogen bonds mediated by a single water molecule (filled by green in Fig. 3a) and His524 binds to a hydroxy group on "D ring" of EST (filled by orange in Fig. 3a). Thus, we followed the policy below for a novel subdividing fragmentation for amino acid residues in a protein and the EST ligand in SBDD context.

First, each amino acid residue of the ER with the conventional fragmentation method is subdivided into main and side chain fragments to discriminate between main or side chain contributions. Fig. 2 shows the fragmentation of the protein for (a) conventional main chain fragmentation and (b) main/side chain fragmentation. A protein is separated at Cα carbon in the conventional main chain fragmentation and that is separated at Cα and Cβ carbons in the novel main/side chain fragmentation. However, Gly (blue) and Pro (green) were not segmented at Cβ and were treated as a single fragment. Additionally, Cys–Cys (red), which is linked by a disulfide bridge, was treated as two main chain fragments and one side chain fragment. We note that, in the fragmentation, the present definition of units of amino acid residues is different from that employed in biochemistry (separated at peptide bonds, i.e., between C=O and N–H), because proteins are divided into fragments at localized orbitals (sp^3) between Cα and the C=O of main chain in the FMO method.

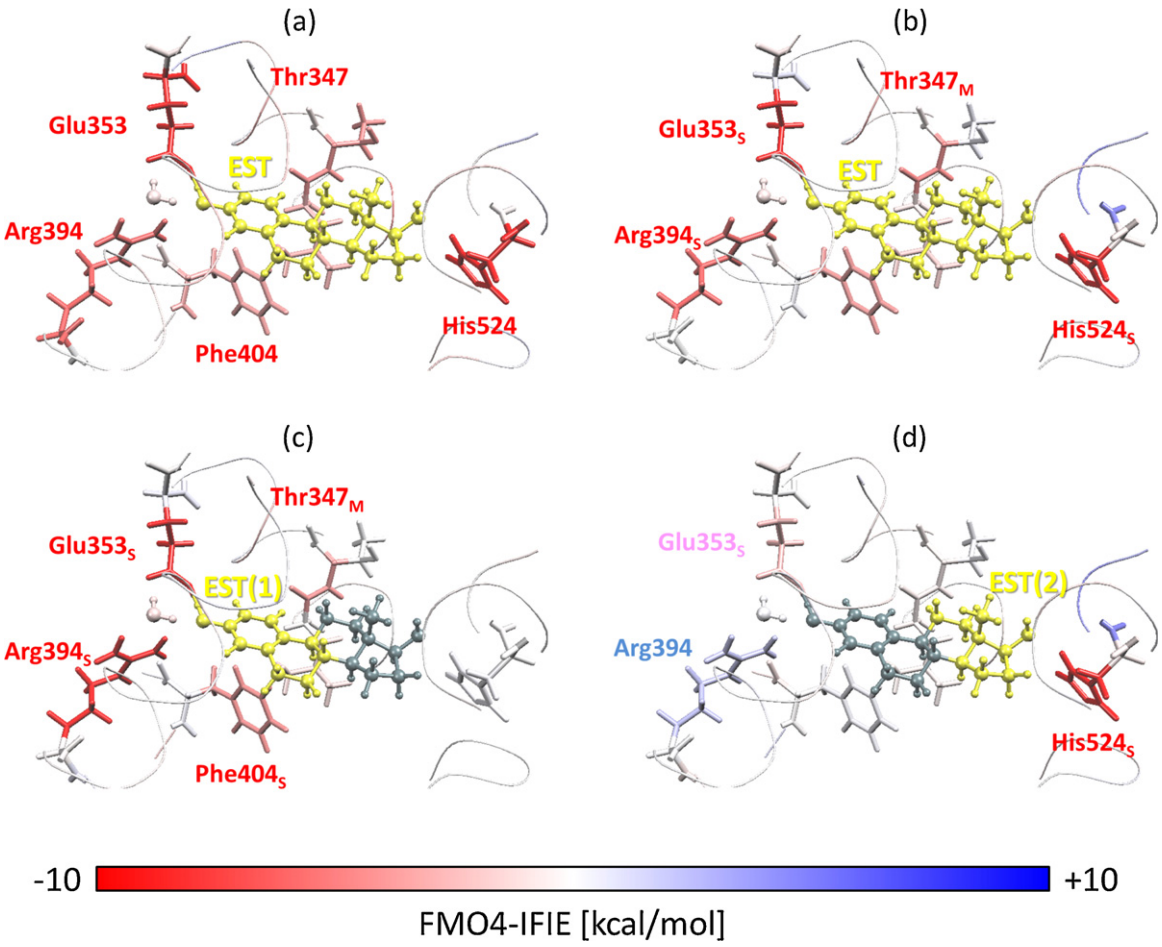

Fig. 4. FMO4-IFIEs between EST and each amino acid of the ER at the MP2/6-31G level: (a) FMO4-IFIEs of EST by the conventional main chain fragmentation, (b) FMO4-IFIEs of EST by the main/side chain fragmentation, (c) FMO4-IFIEs of EST(1) by the main/side chain fragmentation with ligand fragmentation (Model 1), and (d) FMO4-IFIEs of EST(2) by the main/side chain fragmentation with ligand fragmentation (Model 1). The ligand fragments, EST, EST(1), and EST(2), are colored in yellow, and the attractive and repulsive interactions are colored in red and blue, respectively.

Next, the ligand, EST, is here separated into fragments (including "A ring" or "D ring") corresponding to its two ligand-binding sites as illustrated in Fig. 3b. We here use two different fragmentation models (Model 1 and Model 2) to examine whether the total energies and IFIEs depend on the partitioned location of the ligand. The ligand is split into two fragments, EST(1) and EST(2), in units of substructure, which include the cyclohexane ring (designated as the A ring in Fig. 3) and the cyclopentane ring (the D ring shown in Fig. 3) of steroidal EST, respectively.

3. Results and discussion

3.1. Accuracy of the many-body corrected FMO calculations with the novel subdividing fragmentation method for ER-EST complex

The accuracy of the total energy obtained by using FMO2, FMO3, and FMO4 calculations combined with the novel subdividing fragmentations is verified. Here, we perform the many-body corrected FMO calculations with the conventional main chain fragmentation and three novel fragmentation methods: the main chain fragmentation of the protein and divided ligand fragmentation, the main/side chain fragmentation without ligand fragmentation, and the main/side chain combined with ligand fragmentation.

Table 1 lists the total energy errors at the HF/STO-3G level of many-body corrected FMO calculations when the main and main/side chain fragmentations for the protein and the Model 1 and Model 2 fragmentations for ligand are used (see Figs. 2 and 3). In the table, the reference energy value (in units of hartree) is from the conventional MO calculation. We compare the many-body corrected FMO calculations by using the main/side chain fragmentation with the MO calculation to estimate the influence of subdivision in the receptor-protein when ligand fragmentation is not performed (Table 1). The total energy difference in the FMO2 calculation when the main/side chain fragmentations are used is approximately 10.0 hartree, which is not sufficient for chemical accuracy. In contrast, the differences for FMO3 and FMO4 calculations are approximately 10^{-3} hartree; these accuracies are equivalent to that of the FMO4 calculation using the conventional main chain fragmentation. Thus, in the case of main/side chain fragmentation at the HF/STO-3G level, the total energy errors of the FMO3 and FMO4 calculations are within chemical accuracy. These accuracies are maintained even when the ligand is combined with the main/side chain fragmentation (Table 1).

The energy errors are more significant in the many-body corrected FMO calculations at the HF and MP2 levels with 6-31G basis (Table 2). The reference energies (in units of hartree) obtained using the FMO4 calculations with the conventional main chain fragmentation are presented in Table 2. The total energy of the FMO4 calculation is assigned as the reference energy, because a conventional MO calculation of the model protein system (which is composed 50 residues) could not be carried out. We consider the total energy yielded by the FMO4 calculation with

Table 1
Differences in the total energies obtained by the FMO2, FMO3, and FMO4 calculations at HF/STO-3G level using the conventional and novel subdividing fragmentation methods for the ER–EST complex as compared to the conventional MO calculation.

Fragmentation		Difference of total energy (hartree)[c]		
Protein	Ligand	FMO2	FMO3	FMO4
HF/STO-3G (Reference value for total energy: −22578.9472 hartree[c])				
Main chain[a]	No	−0.0215	−0.0038	−0.0048
	Model1	−0.0226	−0.0041	−0.0051
	Model2	−0.0235	−0.0042	−0.0052
Main/side chain[b]	No	−10.1284	0.0020	−0.0073
	Model1	−10.1295	0.0018	−0.0076
	Model2	−10.1304	0.0016	−0.0076

[a] Main chain fragmentation.
[b] Main/side chain fragmentation.
[c] The reference value is obtained using the conventional MO calculation.

conventional main chain fragmentation to be the best effort value. The differences in the total energy with the main/side chain fragmentations are approximately 10.0 and 10^{-2} hartree for the FMO2 and FMO3 calculations, respectively. The differences for the FMO4 results converged to within 10^{-3} hartree, which is equivalent to that of the FMO3 calculation using the conventional main chain fragmentation with 6-31G basis. It is clear that the total energy obtained by the FMO4 calculation with main/side chain fragmentation is chemically accurate at the HF/6-31G and MP2/6-31G levels.

The total energy is unaffected by the inclusion of ligand fragmentation with Model 1 for all levels and basis sets (Tables 1 and 2), and the ligand fragmentation can also be performed without sacrificing chemical accuracy in the FMO2 calculation. The results for Model 1 are similar to those for Model 2, and the total energies of Model 1 and Model 2 are not very different. The total energy is less affected by the differences in the present ligand fragmentation methods, Model 1 and Model 2. Consequently, we find that the accuracy of the total energy depends primarily on the fragmentation scheme used for the protein and is unaffected by the inclusion of the present ligand fragmentation methods (Model 1 and Model 2).

Next, we present an accuracy validation of the IFIEs with many-body corrections at the HF/6-31G and MP2/6-31G levels. Because the properties of the IFIE errors in the HF and MP2 methods are similar, we discuss the IFIEs in the MP2 method. Table 3 lists the many-body corrected IFIEs between EST and each amino acid residue, which is involved in ligand-binding, using the conventional main chain fragmentation, and the differences in the IFIEs between the conventional and the novel subdividing fragmentations. Here, the IFIE value yielded by the novel fragmentation method (the main/side chain fragmentation combined with ligand fragmentation) is expressed by regular fragment units of the conventional main chain fragmentation; a value for each amino acid residue fragment is the sum of the IFIE values of its main and side chain fragments; a value of the ligand is the sum of IFIE values of the EST(1) and EST(2) fragments.

For Model 1 and Model 2, there are four and six amino acids, respectively, for which the differences in FMO2-IFIE exceed 0.5 kcal/mol, and the differences for Leu346 and Phe404 are the largest (1.1 and 1.3 kcal/mol in Model 1 and Model 2, respectively). The six amino acid residues (Leu346, Ala350, Glu353, Leu387, Met388, and Phe404) that have FMO2-IFIE differences greater than 0.5 kcal/mol surround the cleaved region between the EST(1) and EST(2) fragments. Thus, the errors in the FMO2-IFIEs may be caused by alternation in the ligand fragmentation scheme. On the other hand, the differences in the IFIEs are significantly improved by incorporating three- and four-body corrections. For example, the number of residues that have an FMO3-IFIE difference greater than 0.5 kcal/mol is two and three for Model 1 and Model 2, respectively; both values are less than the corresponding values for FMO2-IFIE. There are two amino acids that have an FMO4-IFIE difference

Table 2
Differences in the total energies obtained by the FMO2, FMO3, and FMO4 calculations at several computational levels using the conventional and novel subdividing fragmentation methods for the ER–EST complex.

Fragmentation		Difference of total energy (hartree)[c,d,e]		
Protein	Ligand	FMO2	FMO3	FMO4
HF/STO-3G (Reference value for total energy: −22578.9424 hartree[c])				
Main chain[a]	No[c]	0.0167	−0.0010	–
Main/side chain[b]	No[c]	10.1236	−0.0068	0.0024
	Model1[c]	10.1247	−0.0066	0.0027
	Model2[c]	10.1256	−0.0065	0.0028
HF/6-31G (Reference value for total energy: −22855.8634 hartree[d])				
Main chain[a]	No[d]	−0.0227	0.0032	–
Main/side chain[b]	No[d]	10.0978	−0.0423	−0.0028
	Model1[d]	10.0988	−0.0421	−0.0027
	Model2[d]	10.1007	−0.0420	−0.0028
MP2/6-31G (Reference value for total energy: −22898.2895 hartree[e])				
Main chain[a]	No[e]	−0.0026	−0.0001	–
Main/side chain[b]	No[e]	10.3742	−0.0479	−0.0015
	Model1[e]	10.3776	−0.0461	0.0002
	Model2[e]	10.3797	−0.0462	−0.0001

[a] Main chain fragmentation.
[b] Main/side chain fragmentation.
[c] The reference value is obtained by the FMO4 calculation at HF/STO-3G level with the conventional main chain fragmentation.
[d] The reference value is obtained by the FMO4 calculation at HF/6-31G level with the conventional main chain fragmentation.
[e] The reference value is obtained by the FMO4 calculation at MP2/6-31G level with the conventional main chain fragmentation.

Table 3
Differences of the many-body corrected IFIEs between the conventional and novel subdividing fragmentations. Many-body corrected IFIEs of EST with each amino acid residue obtained by the FMO2, FMO3, and FMO4 calculations.

FMO2-IFIE of EST (kcal/mol)							
Res. #	Res. name	HF/6-31G			MP2/6-31G		
		Reference[a]	Difference[c]		Reference[a]	Difference[c]	
			Model 1[b]	Model 2[b]		Model 1[b]	Model 2[b]
343	Met	−3.12	−0.08	−0.09	−4.93	0.00	−0.01
346	Leu	−0.53	0.80	0.56	−3.35	1.08	0.87
347	Thr	−2.67	0.24	0.33	−4.93	0.36	0.42
350	Ala	−1.30	0.84	0.59	−3.61	1.08	0.78
353	Glu	−38.44	0.53	0.50	−42.10	0.60	0.57
387	Leu	0.47	0.54	0.56	−3.35	0.67	0.74
388	Met	2.03	0.21	0.63	−2.27	0.38	0.91
394	Arg	−5.83	−0.38	−0.26	−7.50	−0.36	−0.24
404	Phe	0.34	−0.14	0.96	−3.92	0.00	1.28
421	Met	−0.55	0.00	−0.05	−2.04	0.18	0.06
524	His	−7.36	0.25	0.09	−11.31	0.44	0.24
Water		−0.67	−0.06	−0.07	−2.02	−0.06	−0.07
FMO2-IFIE sum of EST		−46.28	7.57	8.93	−98.22	11.04	12.59
FMO3-IFIE of EST (kcal/mol)							
Res. #	Res. name	HF/6-31G			MP2/6-31G		
		Reference[a]	Difference[c]		Reference[a]	Difference[c]	
			Model 1[b]	Model 2[b]		Model 1[b]	Model 2[b]
343	Met	−3.07	−0.07	−0.08	−4.88	−0.03	−0.02
346	Leu	−0.49	0.41	0.22	−3.38	0.53	0.35
347	Thr	−2.62	0.30	0.42	−4.98	0.37	0.50
350	Ala	−1.26	0.15	−0.04	−3.64	0.24	0.02
353	Glu	−37.46	0.67	0.63	−40.64	0.72	0.70
387	Leu	0.67	0.10	0.14	−3.13	0.17	0.23
388	Met	2.16	0.15	0.36	−2.27	0.25	0.48
394	Arg	−5.27	−0.37	−0.26	−6.73	−0.36	−0.24
404	Phe	0.39	−0.09	0.40	−3.93	−0.06	0.53
421	Met	−0.54	0.00	−0.05	−2.08	0.17	0.05
524	His	−7.15	0.03	−0.13	−11.12	0.14	−0.06
Water		0.03	−0.05	−0.07	−1.08	−0.06	−0.07
FMO3-IFIE sum of EST		−43.20	2.82	3.44	−95.15	5.01	5.67
FMO4-IFIE of EST (kcal/mol)							
Res. #	Res. name	HF/6-31G			MP2/6-31G		
		Reference[a]	Difference[c]		Reference[a]	Difference[c]	
			Model 1[b]	Model 2[b]		Model 1[b]	Model 2[b]
343	Met	−3.07	−0.07	−0.08	−4.88	−0.03	−0.02
346	Leu	−0.50	0.41	0.20	−3.39	0.54	0.33
347	Thr	−2.63	0.26	0.39	−4.99	0.32	0.47
350	Ala	−1.27	0.17	−0.02	−3.66	0.23	0.03
353	Glu	−37.60	0.64	0.60	−40.83	0.70	0.67
387	Leu	0.64	0.12	0.15	−3.17	0.20	0.26
388	Met	2.14	0.15	0.33	−2.28	0.24	0.44
394	Arg	−5.35	−0.37	−0.26	−6.85	−0.36	−0.24
404	Phe	0.39	−0.09	0.39	−3.92	−0.06	0.52
421	Met	−0.54	0.00	−0.06	−2.08	0.16	0.04
524	His	−7.17	0.03	−0.13	−11.15	0.14	−0.06
Water		−0.10	−0.06	−0.07	−1.27	−0.06	−0.07
FMO4-IFIE sum of EST		−43.74	3.16	3.71	−95.84	5.25	5.85

[a] Conventional main chain fragmentation.

[b] Main/side chain fragmentation combined with the ligand fragmentation given by Model 1 or Model 2.

[c] The reference values are obtained by many-body corrected FMO calculations with the conventional main chain fragmentation.

greater than 0.5 kcal/mol for both Model 1 and Model 2. The difference in FMO4-IFIE for each amino acid almost converges within 1.0 kcal/mol.

In the cases of both Model 1 and Model 2, the difference of the FMO2-IFIE sum obtained using the novel subdividing fragmentation method is greater than 10.0 kcal/mol compared with that obtained using the conventional fragmentation. The differences in the FMO3- and FMO4-IFIE sums, however, converge at approximately 5.0 kcal/mol. Thus, the FMO3- and FMO4-IFIEs obtained by using the novel subdividing fragmentation method for the amino acids and the ligand qualitatively agree with the values obtained by using the conventional fragmentation.

We now compare the accuracy of the different ligand fragmentation schemes, Model 1 and Model 2. The FMO2-IFIE value of Model 1 is preferred over that of Model 2 (see Table 3), although the total energies yielded by Model 1 are similar to those yielded by Model 2 (see Tables 1 and 2). The difference in the FMO3-IFIE values for Model 1 and Model 2 is significantly

less than the difference in the FMO2-IFIE values. The difference in the FMO4-IFIE values for Model 1 and Model 2 is equivalent to the difference in the FMO3-IFIE values. Thus, FMO3- and FMO4-IFIEs could be used to evaluate the interaction energy using ligand fragmentation, in which is separated into two fragments, to characterize a chemical reaction without sacrificing accuracy.

Thus, it is reasonable to use the FMO4 calculation instead of the FMO2 or FMO3 calculation to perform the main/side chain and the ligand fragmentations. Not only FMO4-IFIEs but also FMO3-IFIEs with the novel subdividing fragmentation method enable us to evaluate intermolecular interactions between EST and the ER to within chemical accuracy. Furthermore, there are no significant differences in the ligand fragmentations between Model 1 and Model 2 for both FMO3- and FMO4-IFIEs. Next, we identify the intermolecular interactions between the ER and EST for each ligand-binding site by using the FMO4-IFIE analysis with the main/side chain fragmentation and the ligand fragmentation (Model 1).

3.2. FMO4-IFIE analysis between the ER and EST

Fig. 4 shows the FMO4-IFIEs at MP2/6-31G level of EST with the surrounding residues by using three fragmentation methods: (a) FMO4-IFEs of EST using the conventional main chain fragmentation, (b) FMO4-IFIEs of EST using the main/side chain, (c) FMO4-IFIEs of EST(1) using the main/side chain fragmentation combined with the ligand fragmentation specified in Model 1, and (d) FMO4-IFIEs of EST(2) using the main/side chain fragmentation combined with the ligand fragmentation specified in Model 1; these FMO4-IFIEs at the HF/6-31G and MP2/6-31G levels are listed in Table 4.

The EST fragment (EST, EST(1), and EST(2)) is colored yellow, and the attractive and repulsive interactions are colored red and blue, respectively. The residue name subscripts "M" and "S" designate the main and side chain fragments, respectively (e.g., $Thr347_M$ and $Glu353_S$). We assumed that $\Delta E_{IJ}^{FMO4-HF}$ and $\Delta E_{IJ}^{FMO4-corr}$ ($= \Delta E_{IJ}^{FMO4-MP2} - \Delta E_{IJ}^{FMO4-HF}$) represent contributions of the electrostatic interaction energies, which are originated from electron charges and polarization, and the dispersion interaction energies, which are derived from the vdW, π–π, and CH/π interactions.

In the conventional main chain fragmentation (Fig. 4a and Table 3) for the MP2 method, the EST interacts with Thr347 (−5.0 kcal/mol), Glu353 (−40.8 kcal/mol), Arg394 (−6.9 kcal/mol), Phe404 (−3.9 kcal/mol), and His524 (−11.2 kcal/mol). The previous study that used an identical IFIE analysis [7] concluded that these interactions stem from the strong electrostatic interaction $\Delta E_{IJ}^{FMO4-HF}$ of the surrounding acidic and basic amino acid residues Glu353 (−37.6 kcal/mol), Arg394 (−5.4 kcal/mol), and His524 (−7.2 kcal/mol) through hydrogen bonds, the strong electrostatic interaction $\Delta E_{IJ}^{FMO4-HF}$ of Thr347 (-2.6 kcal/mol), and the dispersion interaction $\Delta E_{IJ}^{FMO4-corr}$ of Phe404 (−4.3 kcal/mol) caused by T-shaped π–π stacking. Although these amino acid residues contribute to protein–ligand binding, we cannot distinguish the contributions of either the main or side chains of amino acid residues; therefore, the origins of these interactions remain unclear. Next, in the main/side chain fragmentation for the MP2 method (Fig. 4b and Table 4), most of the interaction energies of the EST is attributed to interactions with the main chain of Thr347 (−5.4 kcal/mol) and the side chains of Glu535 (−41.7 kcal/mol), Arg394 (−6.8 kcal/mol), Phe404 (−4.3 kcal/mol), and His524 (−10.4 kcal/mol). The interaction of the main chain fragment can be clearly distinguished from that of the side chain fragment by using the main/side chain fragmentation. The FMO4-IFIEs calculated using the fragmentation of amino acids in units of main and side chain fragments alone would not be sufficient for analyzing the intermolecular interactions between the ER and EST for each ligand-binding site in the functional unit. Furthermore, the ligand-binding mechanism of the ER can be elucidated by analyzing the interactions between each functional group of EST and either the main or side chain of each amino acid residue shown in Fig. 4c and d. In the MP2 method (Fig. 4c and Table 4), EST(1) mainly interacts with the main chain of Thr347 (−4.5 kcal/mol) and the side chains of Glu353 (−38.0 kcal/mol), Arg394 (−9.6 kcal/mol), and Phe404 (−4.8 kcal/mol). The strong interactions of EST(1) with the side chains of Glu353 and Arg394 stem from the respective electrostatic interaction energies $\Delta E_{IJ}^{FMO4-HF}$ of −34.8 and −8.1 kcal/mol, which are primarily due to their hydrogen bonds, as observed in Fig. 3a. The interaction between EST(1) and the main chain of Thr347 is mainly the electrostatic interaction $\Delta E_{IJ}^{FMO4-HF}$ (−3.2 kcal/mol), which is a results of the polarization of the main chain. The interaction between EST(1) and the side chain of Phe404 is mainly contributed by the dispersion interaction energy $\Delta E_{IJ}^{FMO4-corr}$ (−3.9 kcal/mol), which results from the π–π and CH/π interactions. Undivided EST in the conventional way totally shows the electrostatic interaction with His524, however, its divided part, EST(1), do not have such the attractive interaction indeed. On the other hand, the another part, EST(2), interacts primarily with the side chain of His524 and its interaction energy is −10.6 kcal/mol at the MP2 level (Fig. 4d and Table 4). The identification of binding affinity for each functional units of ligand is one of new findings obtained from our novel fragmentation method and FMO4-IFIE analysis. The interaction of EST(2) with the side chain of His524 mainly stems from the electrostatic interaction energy $\Delta E_{IJ}^{FMO4-HF}$ (−6.9 kcal/mol), which is due to their hydrogen bond, as can be observed from Fig. 3a. Thus, the intermolecular interactions between the ER and EST at each ligand-binding site (Fig. 3a) are specified by the FMO4-IFIE analysis using the novel subdividing fragmentation method. Moreover, binding affinities in functional units of EST are revealed by the FMO4-IFIE analysis and the origin of these interactions is more apparent. These findings cannot be obtained by FMO2-IFIE analysis with the conventional main chain fragmentation.

Not only strong electrostatic interactions (e.g., hydrogen bonds) but also weak electron correlation interactions (e.g., CH/π bonds) play key roles in protein–ligand binding and protein folding through intermolecular and intramolecular bonding. The IFIE values for the dispersion and vdW interactions are assessed by the complicated FILM analysis [38] because conventional FMO2-IFIE analysis by using the MP2 method cannot sufficiently characterize these weak electron correlation interactions. We then introduce the FMO4-IFIE analysis by using the MP2 method with the novel subdividing fragmentation as a simple approach to identify CH/π interactions, as demonstrated in the scheme described below.

An exhaustive search for CH/π hydrogen bonds was performed by using the CHPI program available in BioStation Viewer. This program searches the distances and angles between CHs and interacting aromatic rings by using structural information derived from X-ray crystallography and input from PDB files. Here, the CH/π interaction between the ER and EST is identified by both the quantitative estimation of the FMO4-IFIE values using our novel subdividing fragmentation method and the exhaustive searching using the CHPI program.

CH/π hydrogen bonds are detected by using the CHPI program. There are three CH/π hydrogen bonds between the aromatic ring of EST (the A ring) and the CHs of Ala350, Leu387, and Phe404 (Fig. 5). Hence, intermolecular interactions of EST(1) with Ala350, Leu387, and Phe404 are analyzed by FMO4-IFIEs with our novel subdividing fragmentation method at the HF and MP2 levels. Not only the electrostatic but also the dispersion interactions are incorporated into IFIEs by the MP2 method. Here, we assume that $\Delta E_{IJ}^{FMO4-HF}$

Table 4
Four-body corrected IFIEs of EST with each amino acid residue with the novel subdividing fragmentation method for the ER and EST complex.

FMO4-IFIE of EST (kcal/mol)								
Res. #	Res. name	Main/side chain	HF/6-31G			MP2/6-31G		
			Fragmentation of ligand			Fragmentation of ligand		
			No[a]	Model 1[b]		No[a]	Model 1[b]	
			EST	EST(1)	EST(2)	EST	EST(1)	EST(2)
343	Met	Main	−0.48	0.04	−0.57	−0.57	0.04	−0.64
		Side	−2.62	0.39	−3.00	−4.33	0.33	−4.64
346	Leu	Main	−0.63	0.00	−0.37	−1.10	−0.26	−0.58
		Side	0.28	−0.25	0.54	−2.06	−1.45	−0.56
347	Thr	Main	−3.34	−3.20	0.10	−5.42	−4.51	−0.63
		Side	0.84	0.19	0.54	0.58	0.14	0.33
350	Ala	Main	−2.50	−1.69	−0.82	−3.58	−2.64	−0.94
		Side	1.26	0.80	0.61	0.00	−0.18	0.34
353	Glu	Main	1.05	0.89	0.14	1.00	0.84	0.14
		Side	−38.54	−34.83	−3.16	−41.74	−37.96	−3.16
394	Arg	Main	−0.12	−0.31	0.18	−0.12	−0.31	0.18
		Side	−5.29	−8.14	2.55	−6.79	−9.63	2.55
404	Phe	Main	0.45	0.64	−0.16	0.35	0.55	−0.16
		Side	−0.06	−0.86	0.67	−4.27	−4.79	0.41
524	His	Main	−0.63	0.09	−0.70	−0.83	0.09	−0.89
		Side	−6.61	0.37	−6.90	−10.35	0.37	−10.58
	Water		−0.09	−0.40	0.24	−1.26	−1.57	0.24
	FMO4-IFIE sum		−41.66	−38.77	−1.80	−92.89	−67.84	−22.75

[a] Main/side chain fragmentation.
[b] Main/side chain fragmentation combined with the ligand fragmentation given by Model 1.

and $\Delta E_{IJ}^{\mathrm{FMO4-corr}}$ represent the contributions of the electrostatic interaction energies, which result from the electron charges and polarization, and the dispersion interaction energies, which derive from the CH/π hydrogen bond. Under this assumption, we calculate the dispersion interaction energies of CH/π interactions by using the FMO4-IFIE analysis and discuss the validity of these results.

Fig. 6a and b use color to illustrate the FMO4-IFIE of EST with each amino acid residue fragment of the ER calculated by using conventional main chain fragmentation. Ala350 interact with EST(1) through electrostatic interaction (−1.3 kcal/mol) at the HF level. In contrast, the interaction energy at the MP2 level through dispersion interaction is −3.7 kcal/mol, which is more stable than that at the HF level. By using the HF method, we determine that Leu387 and Phe404 have repulsive interactions with EST with energies of 0.6 and 0.4 kcal/mol, respectively. The interaction energies yielded by the MP2 method, −3.2 and −3.9 kcal/mol, are more attractive.

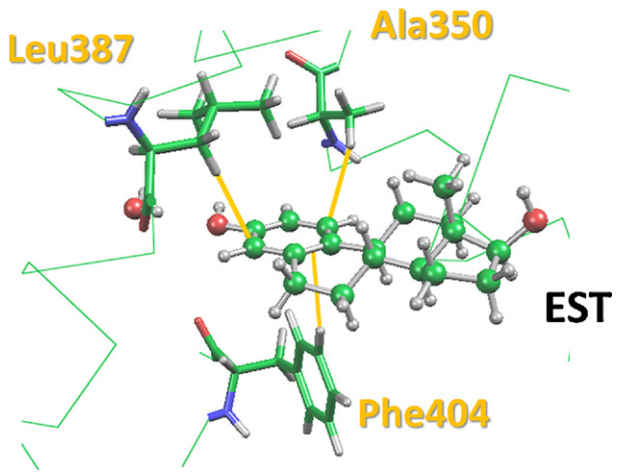

Fig. 5. CHPI analysis between the ER and EST. The orange solid lines indicate CH/π hydrogen bonds founded by CHPI program. (For interpretation of the references to color in the artwork, the reader is referred to the web version of the article.)

IFIE cannot distinguish whether the contributions are either main chain or side chain when the conventional fragmentation in units of residues and ligand is used. Thus, it is difficult to quantitatively identify the CH/π interaction.

To enable the identification of dispersion interaction for the CH/π interaction, we use the FMO4-IFIE analysis with our novel subdividing fragmentation method. Fig. 6c and d demonstrate that EST(1) mostly interacts with the main chain of Ala350; its interaction is almost originated from the electrostatic interaction energy $\Delta E_{IJ}^{\mathrm{FMO4-HF}}$ (−1.7 kcal/mol), and its electron correlation energy $\Delta E_{IJ}^{\mathrm{FMO4-corr}}$ is weakly attractive (−1.0 kcal/mol). EST(1) does not interact with the side chain of Ala350 through either electrostatic or dispersion interactions. Next, the intermolecular interaction between EST(1) and the main chain of Leu387 is assigned attractive interactions, with energies of −0.8 and −1.1 kcal/mol, by the HF and MP2 methods, respectively. Since the dispersion interaction $\Delta E_{IJ}^{\mathrm{FMO4-corr}}$ had very small energy (−0.3 kcal/mol), the intermolecular interaction largely depends on the electrostatic interaction. Although the side chain of Leu387 has a repulsive electrostatic interaction (1.4 kcal/mol) at the HF level, the interaction energy of the side chain of Leu387 at the MP2 level becomes attractive (−1.9 kcal/mol) by dispersion interaction (−3.3 kcal/mol) which results from the CH/π interaction. Finally, EST(1) does not interact with the main chain of Phe404 through either the electrostatic or dispersion interactions. The side chain of Phe404 has a weak attractive interaction with EST(1) by the HF method (−0.9 kcal/mol). However, the interaction energy yielded by the MP2 method became more attractive (−4.8 kcal/mol); this interaction is originated from the dispersion interaction (−3.9 kcal/mol) of CH/π and π–π interactions.

Since the stabilization energy in the protein system is about −1.5 to −2.5 kcal/mol per CH/π interaction, the number of CH/π interactions that occur in the ER–EST complex was evaluated by the numerical estimation with the FMO4-IFIEs and a conformational search performed by the CHPI program [31,37]. For example, from the position of the CHs of Phe404 and the aromatic ring of EST(1), Phe404 will have two or three CH/π interactions, although the CHPI program detected only one CH/π hydrogen bond for Phe404.

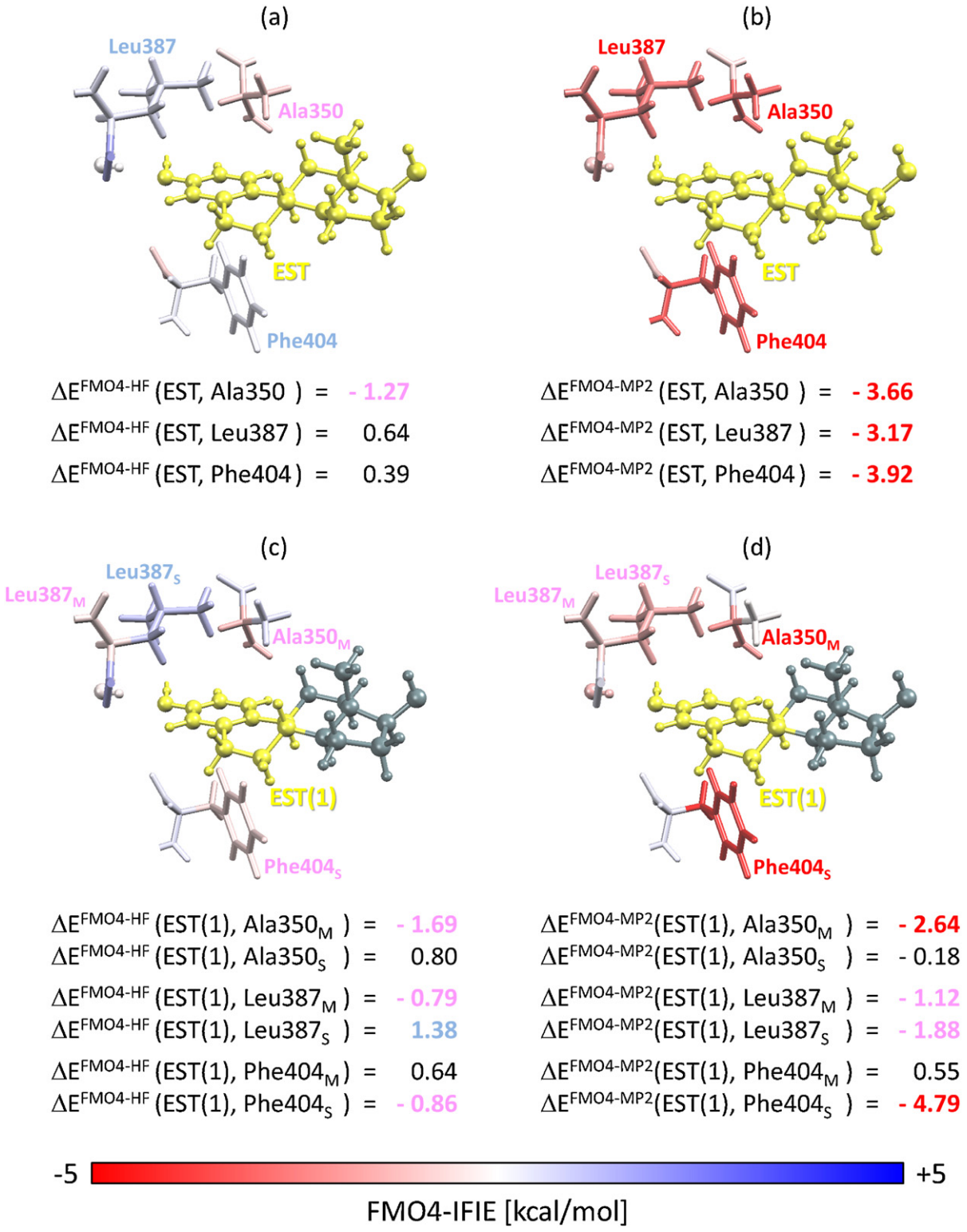

Fig. 6. FMO4-IFIEs at the HF/6-31G and MP2/6-31G levels of EST(1) for the specified CH/π interactions: (a) and (b) the conventional main chain fragmentation, (c) and (d) the novel main/side chain fragmentation with ligand fragmentation (Model 1). EST(1) is colored in yellow, and the attractive and repulsive interactions are colored in red and blue, respectively. (For interpretation of the references to color in the artwork, the reader is referred to the web version of the article.)

Additionally, observation of their positions suggests that the phenyl group of Phe404 and the "A ring" of EST(1) may form a T-shaped π–π interaction. The results are in agreement with the results of an analysis by FILM at the molecular orbital level, which found two CH/π interactions and one π–π interaction between Phe404 and EST [2].

Considering the FMO4-IFIEs estimated by using our novel subdividing fragmentation method combined with a search performed the CHPI program, Leu387 and Phe404 must interact with the "A ring" of EST through CH/π and T-shaped π–π interactions, respectively. Moreover, we must modify the previous assignment of intermolecular interactions between Ala350 and EST by using

conventional fragmentation. It is clear that Ala350 does not form a CH/π interaction with EST because the main chain of Ala350 mainly contributes to the stabilization of the EST binding mechanism by electrostatic interaction, as indicated by the FMO4-IFIEs. The stabilization of EST with Leu387 is derived from both the polarization of the main chain and the CH/π interaction of the side chain. It is reasonable to suppose that Phe404 has an attractive interaction with EST that originates from a few CH/π interactions and a T-shaped π–π interaction.

From these results, intermolecular interactions between the ER and EST in a functional unit have been confirmed by a high-resolution analysis using FMO4-IFIEs with our novel subdividing fragmentation method, which is more detailed than the conventional fragmentation. Additionally, it is easier to identify CH/π interactions by using cooperation between the FMO4-IFIEs with our novel subdividing fragmentation method and the CHPI program, although these interactions have not yet been sufficiently evaluated by using FMO2-IFIEs with conventional main chain fragmentation.

4. Summary and conclusions

The FMO4 calculation with our novel subdividing fragmentation method for amino acid residues and ligand was performed for the ER–EST complex to quantitatively reveal the key functional units of amino acid residues (main and side chains) and substructures of a ligand (EST(1) and EST(2)) having important roles in the ligand-binding mechanism. In order to subdivide fragments into smaller ones, we examined the accuracies of total energy and IFIEs by using FMO2, FMO3, and FMO4 calculations. It was confirmed that the total energy of the FMO4 calculation is more accurate than those of the FMO2 and FMO3 calculations (Table 2). On the other hand, the FMO3- and FMO4-IFIEs with the novel subdividing fragmentation method offer accuracy comparable to those of IFIEs with the conventional fragmentation, which may be ascribable to this ligand fragmentation divided into two fragments (Table 3).

The FMO4-IFIEs between the ER and EST revealed that EST(1), which includes the "A ring" of EST, interacts with the main chain of Thr347 that originated from the polarization of the main chain and with the side chains of Glu353 and Arg349 derived from hydrogen bonds; EST(2), which includes the "D ring" of EST, interacts primarily with the side chain of His524 owing to the hydrogen bond. Based on cooperation between the FMO4-IFIE analysis with the novel subdividing fragmentation method and the CHPI program, we clearly demonstrated that the side chains of Leu387 and Phe404 have attractive interactions with EST(1) derived from CH/π and T-shaped π–π interactions, whereas the side chain of Ala350, which is detected as a CH/π hydrogen bond by the CHPI program, does not interact with EST(1). Thus, binding affinity in functional units of EST is revealed by the FMO4-IFIE analysis and the origin of these interactions is more apparent.

It was found that the FMO4 calculation with our novel subdividing fragmentation method is available for analysis of intermolecular interactions for each ligand-binding site in SBDD context. In addition, the cooperation between the FMO4-IFIE analysis by using the our novel subdividing fragmentation method and the CHPI program will be useful to specify weak interactions, such as the CH/π interaction, in units of functional group. While we have confirmed that the FMO3-IFIEs are mostly in agreement with the FMO4-IFIEs, it may be a particular case owing to the present fragmentation, where EST is separated into two fragments. Thus, we would like to extend these analyses by splitting ligands with several ligand-binding sites into three or more fragments for rational drug design such as SBDD and FBDD [29,30] and by dividing peptides and proteins into units of biochemical amino acid residues [44]. We will need to examine whether chemical properties of a minimum model protein, which was used in this study, are in qualitative agreement with those of a full model protein. Hence, the Cholesky decomposition [45] and the ESP approximation [3] approaches as high-speed computational methods will be necessary to execute FMO4 calculations for large system in order to efficiently reduce the computational cost. The verification of the FMO4 calculation with/without these approaches is an important future work.

Altogether, the FMO4-IFIE analysis using our novel subdividing fragmentation method, which divides a ligand into functional group units and amino acid residues into main and side chain fragments, is a useful tool to elucidate the details of ligand-binding mechanism and will be applicable to rational drug design using methods such as SBDD and FBDD.

Acknowledgements

The authors would like to thank Mr. Katsumi Yamashita for technical support and Dr. Motohiro Nishio and Dr. Yoji Umezawa for valuable discussions when preparing the manuscript. This research was done in the "Research and Development of Innovative Simulation Software" project supported by Research and Development for Next-generation Information Technology of the Ministry of Education, Culture, Sports, Science and Technology (MEXT). Finally, YM and KF acknowledge the SFR-aid provided by Rikkyo University.

References

[1] K. Kitaura, E. Ikeo, T. Asada, T. Nakano, M. Uebayasi, Fragment molecular orbital method: an approximate computational method for large molecules, Chemical Physics Letters 313 (1999) 701–706.
[2] D.G. Fedorov, K. Kitaura, The Fragment Molecular Orbital Method: Practical Application to Large Molecular Systems, CRC Press, Bica Raton, FL, 2009.
[3] T. Nakano, T. Kaminuma, T. Sato, K. Fukuzawa, Y. Akiyama, M. Uebayasi, K. Kitaura, Fragment molecular orbital method: use of approximate electrostatic potential, Chemical Physics Letters 351 (2002) 475–480.
[4] D.G. Fedorov, K. Kitaura, Extending the power of quantum chemistry to large systems with the fragment molecular orbital method, Journal of Physical Chemistry A 111 (2007) 6904–6914.
[5] D.G. Fedorov, T. Nagata, K. Kitaura, Exploring chemistry with the fragment molecular orbital method, Physical Chemistry Chemical Physics 14 (2012) 7562–7577.
[6] K. Fukuzawa, K. Kitaura, M. Uebayasi, K. Nakata, T. Kaminuma, T. Nakano, Ab initio quantum mechanical study of the binding energies of human estrogen receptor with its ligands: an application of fragment molecular orbital method, Journal of Computational Chemistry 26 (2005) 1–10.
[7] K. Fukuzawa, Y. Mochizuki, S. Tanaka, K. Kitaura, T. Nakano, Molecular interactions between estrogen receptor and its ligand studied by the ab initio fragment molecular orbital method, Journal of Physical Chemistry B 110 (2006) 16102–16110.
[8] M. Ito, K. Fukuzawa, Y. Mochizuki, T. Nakano, S. Tanaka, Ab initio fragment molecular orbital study of molecular interactions between liganded retinoid X receptor and its coactivator: roles of helix 12 in the coactivator binding mechanism, Journal of Physical Chemistry B 111 (2007) 3525–3533.
[9] M. Ito, K. Fukuzawa, Y. Mochizuki, T. Nakano, S. Tanaka, Ab initio fragment molecular orbital study of molecular interactions between liganded retinoid x receptor and its coactivator; Part II: influence of mutations in transcriptional activation function 2 activating domain core on the molecular interactions, Journal of Physical Chemistry A 112 (2008) 1986–1998.
[10] M. Ito, K. Fukuzawa, T. Ishikawa, Y. Mochizuki, T. Nakano, S. Tanaka, Ab initio fragment molecular orbital study of molecular interactions in liganded retinoid x receptor: specification of residues associated with ligand inducible information transmission, Journal of Physical Chemistry B 112 (2008) 12081–12094.
[11] K. Yamagishi, K. Yamamoto, S. Yamada, H. Tokiwa, Functions of key residues in the ligand-binding pocket of vitamin D receptor: fragment molecular orbital–interfragment interaction energy analysis, Chemical Physics Letters 420 (2006) 465–468.
[12] K. Yamagishi, K. Yamamoto, Y. Mochizuki, T. Nakano, S. Yamada, H. Tokiwa, Flexible ligand recognition of peroxisome proliferator-activated receptor-γ (PPARγ), Bioorganic and Medicinal Chemistry Letters 20 (2010) 3344–3347.
[13] T. Ozawa, K. Okazaki, CH/π hydrogen bonds determine the selectivity of the Src homology 2 domain to tyrosine phosphotyrosyl peptides: an ab initio fragment molecular orbital study, Journal of Computational Chemistry 29 (2008) 2656–2666.

[14] T. Ozawa, E. Tsuji, M. Ozawa, C. Handa, H. Mukaiyama, T. Nishimura, S. Kobayashi, K. Okazaki, The importance of CH/π hydrogen bonds in rational drug design: an ab initio fragment molecular orbital study to leukocyte-specific protein tyrosine (LCK) kinase, Bioorganic and Medicinal Chemistry 16 (2008) 10311–10318.
[15] T. Ozawa, K. Okazaki, K. Kitaura, CH/π hydrogen bonds play a role in ligand recognition and equilibrium between active and inactive states of the b2 adrenergic receptor: An ab initio fragment molecular orbital (FMO) study, Bioorganic and Medicinal Chemistry 19 (2011) 5231–5237.
[16] T. Ozawa, K. Okazaki, K. Kitaura, Importance of CH/π hydrogen bonds in recognition of the core motif in proline-recognition domains: an ab initio fragment molecular orbital study, Journal of Computational Chemistry 32 (2011) 2774–2782.
[17] K. Fujimura, Y. Sasabuchi, The role of fluorine atoms in a fluorinated prostaglandin agonist, ChemMedChem 5 (2010) 1254–1257.
[18] K. Ohno, K. Mori, M. Orita, M. Takeuchi, Computational insights into binding of bisphosphates to farnesyl pyrophosphate synthase, Current Medicinal Chemistry 18 (2011) 220–233.
[19] O. Ichihara, J. Barker, R.J. Law, M. Whittaker, Compound design by fragment-linking, Molecular Informatics 30 (2011) 298–306.
[20] M.P. Mazanetz, O. Ichihara, R.J. Law, M. Whittaker, Prediction of cyclin-dependent kinase 2 inhibitor potency using the fragment molecular orbital method, Journal of Cheminformatics 3 (2011) 2.
[21] J. Vermot, J.G. Llamas, V. Fraulob, K. Niederreither, P. Chambon, P. Dollé, Retinoic acid controls the bilateral symmetry of somite formation in the mouse embryo, Science 308 (2005) 563–566.
[22] K.B. Horwitz, W.L. McGuire, Estrogen control of progesterone receptor in human breast cancer. correlation with nuclear processing of estrogen receptor, Journal of Biological Chemistry 253 (1978) 2223–2228.
[23] A. Berkenstam, J.-Å. Gustafsson, Nuclear receptors and their relevance to diseases related to lipid metabolism, Current Opinion in Pharmacology 5 (2005) 171–176.
[24] J.T. Moore, J.L. Collins, K.H. Pearce, The nuclear receptor superfamily and drug discovery, ChemMedChem 1 (2006) 504–523.
[25] T. Kaminuma, Pathways and networks of nuclear receptors and modeling of syndrome X, Chem-Bio Informatics Journal 3 (2003) 130–156.
[26] I.D. Kuntz, Structure-based strategies for drug design and discovery, Science 257 (1992) 1078–1082.
[27] M. von Itzstein, W.-Y. Wu, G.B. Kok, M.S. Pegg, J.C. Dyason, B. Jin, T. van Phan, M.L. Smythe, H.F. White, S.W. Oliver, P.M. Colman, J.N. Varghese, D.M. Ryan, J.M. Woods, R.C. Bethell, V.J. Hotham, J.M. Cameron, C.R. Penn, Rational design of potent sialidase-based inhibitors of influenza virus replication, Nature 363 (1993) 418–423.
[28] K. Raha, M.B. Peters, B. Wang, N. Yu, A.M. Wollacott, L.M. Westerhoff, K.M. Merz Jr., The role of quantum mechanics in structure-based drug design, Drug Discovery Today 12 (2007) 725–731.
[29] S. Hitaoka, M. Harada, T. Yoshida, H. Chuman, Correlation analyses on binding affinity of sialic acid analogues with influenza virus neuraminidase-1 using ab initio MO calculations on their complex structures, Journal of Chemical Information and Modeling 50 (2010) 1796–1805.
[30] S. Hitaoka, H. Matoba, M. Harada, T. Yoshida, D. Tsuji, T. Hirokawa, K. Itoh, H. Chuman, Correlation analyses on binding affinity of sialic acid analogues and anti-influenza drugs with human neuraminidase using ab initio MO calculations on their complex structures-LERE-QSAR analysis (IV), Journal of Chemical Information and Modeling 51 (2011) 2706–2716.
[31] Y. Umezawa, M. Nishio, CH/π interactions as demonstrated in the crystal structure of guanine-nucleotide binding proteins, src homology-2 domains and human growth hormone in complex with their specific ligands, Bioorganic and Medicinal Chemistry 6 (1998) 493–504.
[32] Y. Umezawa, M. Nishio, CH/π interactions in the crystal structure of class I MHC antigens and their complexes with peptides, Bioorganic and Medicinal Chemistry 6 (1998) 2507–2515.
[33] Y. Umezawa, M. Nishio, CH/π interactions in the crystal structure of TATA-box binding protein/DNA complexes, Bioorganic and Medicinal Chemistry 8 (2000) 2643–2650.
[34] Y. Umezawa, M. Nishio, CH/π hydrogen bonds as evidenced in the substrate specificity of acetylcholine esterase, Biopolymers 79 (2005) 248–258.
[35] M. Nishio, The CH/π hydrogen bond in chemistry. Conformation, supramolecules, optical resolution and interactions involving carbohydrates, Physical Chemistry Chemical Physics 13 (2011) 13873–13900.
[36] M. Brandl, M.S. Weiss, A. Jabs, J. Sühnel, R. Hilgenfeld, C—H···π-interactions in proteins, Journal of Molecular Biology 307 (2001) 357–377.
[37] BioStation 5.0: ABINIT-MP and BioStation Viewer. The program package is available at: http://www.ciss.iis.u-tokyo.ac.jp/english/dl/
[38] T. Ishikawa, Y. Mochizuki, S. Amari, T. Nakano, H. Tokiwa, S. Tanaka, K. Tanaka, Fragment interaction analysis based on local MP2, Theoretical Chemistry Accounts 118 (2007) 937–945.
[39] T. Nakano, Y. Mochizuki, K. Yamashita, C. Watanabe, K. Fukuzawa, K. Segawa, Y. Okiyama, T. Tsukamoto, S. Tanaka, Development of the four-body corrected fragment molecular orbital (FMO4) method, Chemical Physics Letters 523 (2012) 128–133.
[40] R. Law, O. Barker, J.J. Barker, T. Hesterkamp, R. Godemann, O. Andersen, T. Fryatt, S. Courtney, D. Hallett, M. Whittaker, The multiple roles of computational chemistry in fragment-based drug design, Journal of Computer Aided Molecular Design 23 (2009) 459–473.
[41] M. Whittaker, R.J. Law, O. Ichihara, T. Hesterkamp, D. Hallett, Fragments: past, present and future, Drug Discovery Today: Technologies 7 (2010) e163–e171.
[42] Y. Mochizuki, K. Yamashita, T. Murase, T. Nakano, K. Fukuzawa, K. Takematsu, H. Watanabe, S. Tanaka, Large scale FMO-MP2 calculations on a massively parallel-vector computer, Chemical Physics Letters 457 (2008) 396–403.
[43] This program is a development version of BioStation 5.0 in Reference [37].
[44] A. Yoshioka, K. Takematsu, I. Kurisaki, K. Fukuzawa, Y. Mochizuki, T. Nakano, E. Nobusawa, K. Nakajima, S. Tanaka, Antigen–antibody interactions of influenza virus hemagglutinin revealed by the fragment molecular orbital calculation, Theoretical Chemistry Accounts 130 (2011) 1197–1202.
[45] Y. Okiyama, T. Nakano, K. Yamashita, Y. Mochizuki, N. Taguchi, S. Tanaka, Acceleration of fragment molecular orbital calculations with Cholesky decomposition approach, Chemical Physics Letters 490 (2010) 84–89.